Huntwork-Rodriguez et al., http://www.jcb.org/cgi/content/full/jcb.201303066/DC1

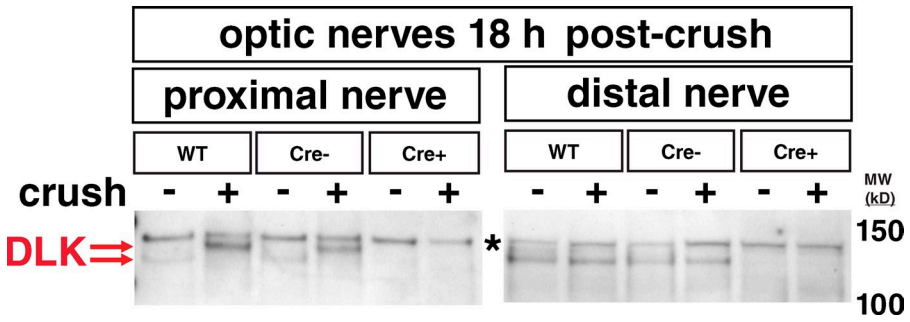

Figure S1. **Additional description of DLK blots shown in Fig. 3.** Nerve crush was performed on mice of the given genotypes and nerves were collected 18 h later. WT, C57BL/6. Cre-, $Dlk^{lox/lox}$; Cre^{-}. Cre+, $DLK^{lox/lox}$; Cre^{+}. *Dlk* conditional knockouts treated with tamoxifen (Cre+) were used to determine which bands were specific for DLK. Red arrows point to low molecular weight and high molecular weight DLK. *, background band.

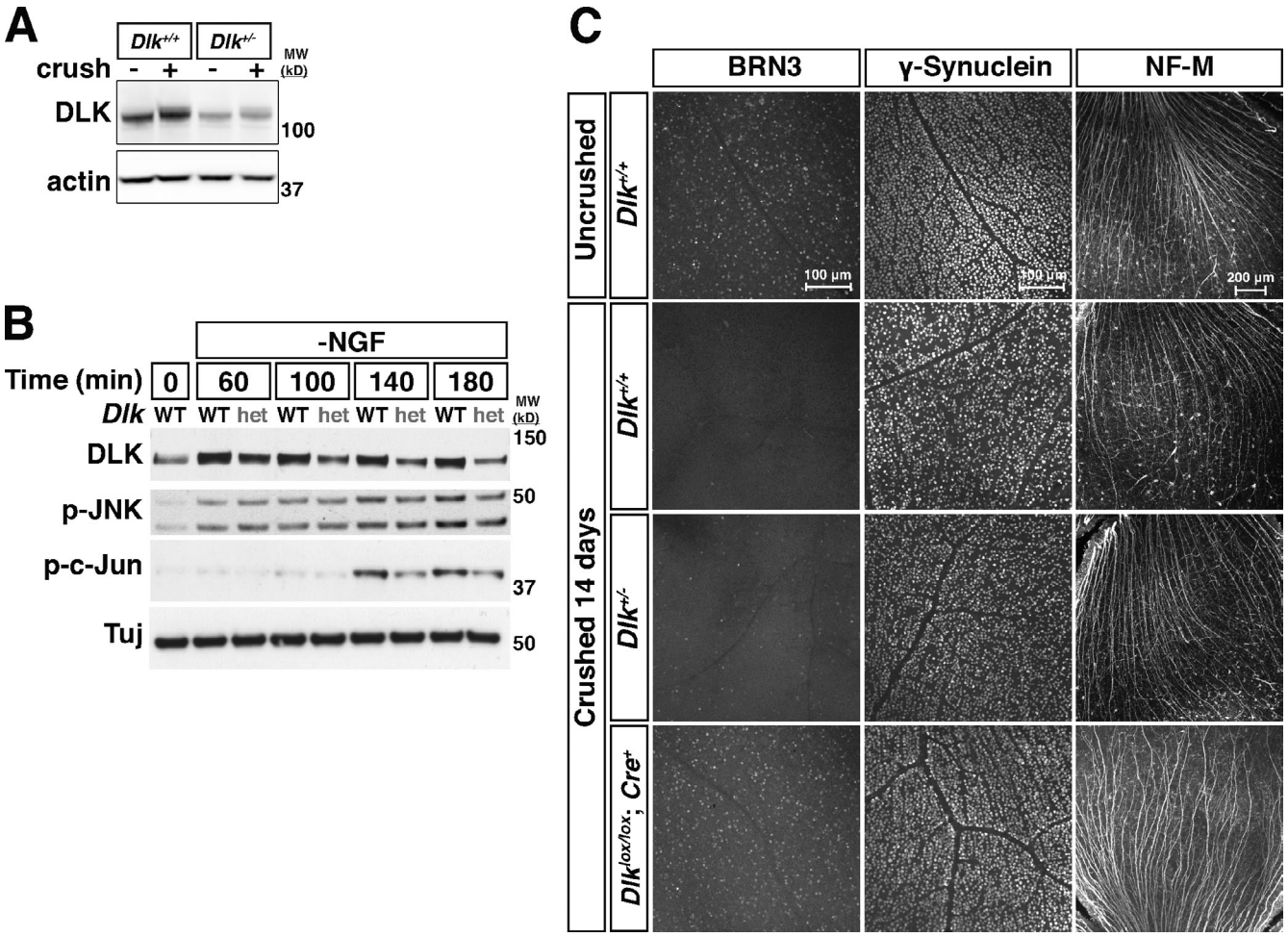

Figure S2. **Further characterization of JNK signaling and neurodegeneration in *Dlk* heterozygotes.** (A) Retinas from $Dlk^{+/+}$ (wild type) and $Dlk^{+/-}$ (heterozygous) mice show that heterozygous retinas contain approximately half the DLK of wild-type retinas in both uncrushed and crushed samples. (B) A time course of trophic factor withdrawal in $Dlk^{+/+}$ (WT) and $Dlk^{+/-}$ (het) DRGs reveals that the reduction of DLK protein levels in heterozygous neurons results in reduced phosphorylation of the downstream targets JNK and c-Jun. (C) Staining for BRN3, γ-synuclein, and neurofilament-M (NF-M) at two weeks post-crush in *Dlk* WT, heterozygous, and conditional knockout retinas compared with uncrushed wild-type controls.

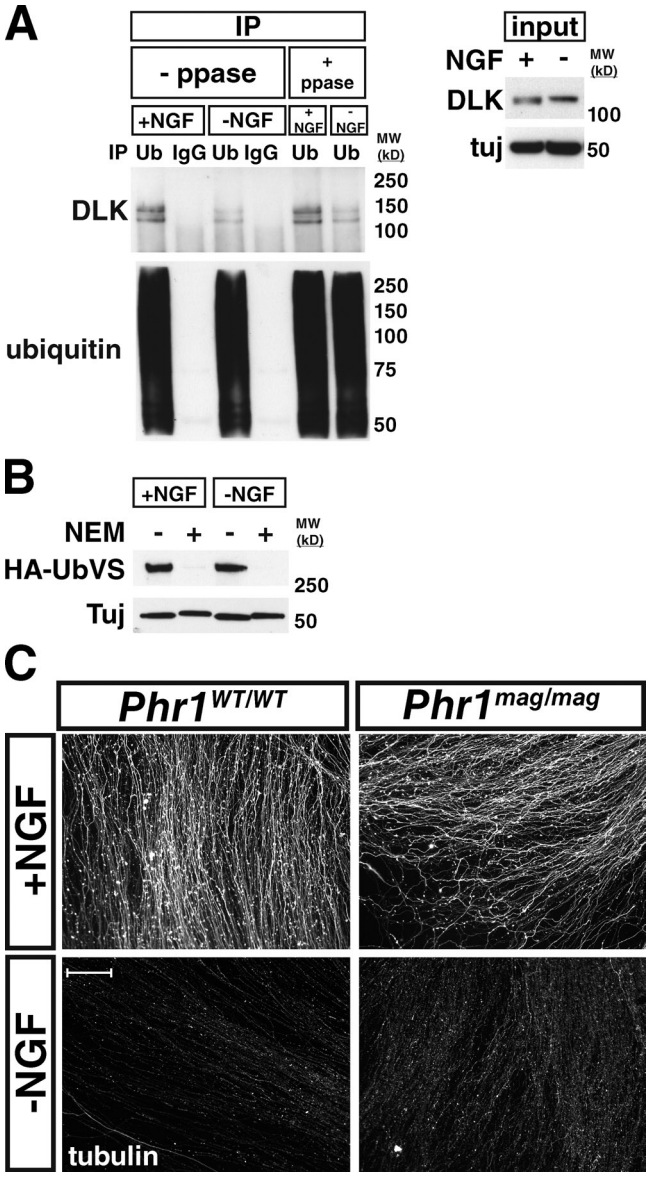

Figure S3. **Additional analysis of USP9X and PHR1 function.** (A) Treatment of anti-ubiquitin immunoprecipitates with lambda protein phosphatase (+ ppase) does not alter the migration of DLK. This demonstrates that the DLK doublet seen with anti-ubiquitin immunoprecipitation is not the product of different phosphorylated forms of DLK. (B) USP9X activity does not change with trophic factor withdrawal. Incubation of + and −NGF-treated DRG lysates with HA-tagged ubiquitin vinyl sulfones (HA-UbVS), which covalently and irreversibly bind to the active site of de-ubiquitinating enzymes (DUBs), shows no change in USP9X activity with trophic factor withdrawal. Lysates incubated with HA-tagged ubiquitin vinyl sulfones were run on an SDS-PAGE gel and then blotted with an anti-HA antibody. HA epitope detected at ~290 kD is due to covalent binding to USP9X, and the amount of HA detected is determined by the activity of USP9X. See also Borodovsky et al. (2002). *N*-ethylmaleimide (NEM), which inhibits DUBs, is used as a negative control. (C) No effect of loss of function of PHR1 on degeneration of sensory neuron axons 18 h after NGF withdrawal. Embryonic DRGs were cultured from *Phr1*$^{WT/WT}$ or *Phr1*$^{mag/mag}$ littermate embryos and deprived of NGF after 3 d in vitro. 18 h later, both cultures were equally degenerated, as visualized by tubulin staining. Bar, 100 µm.

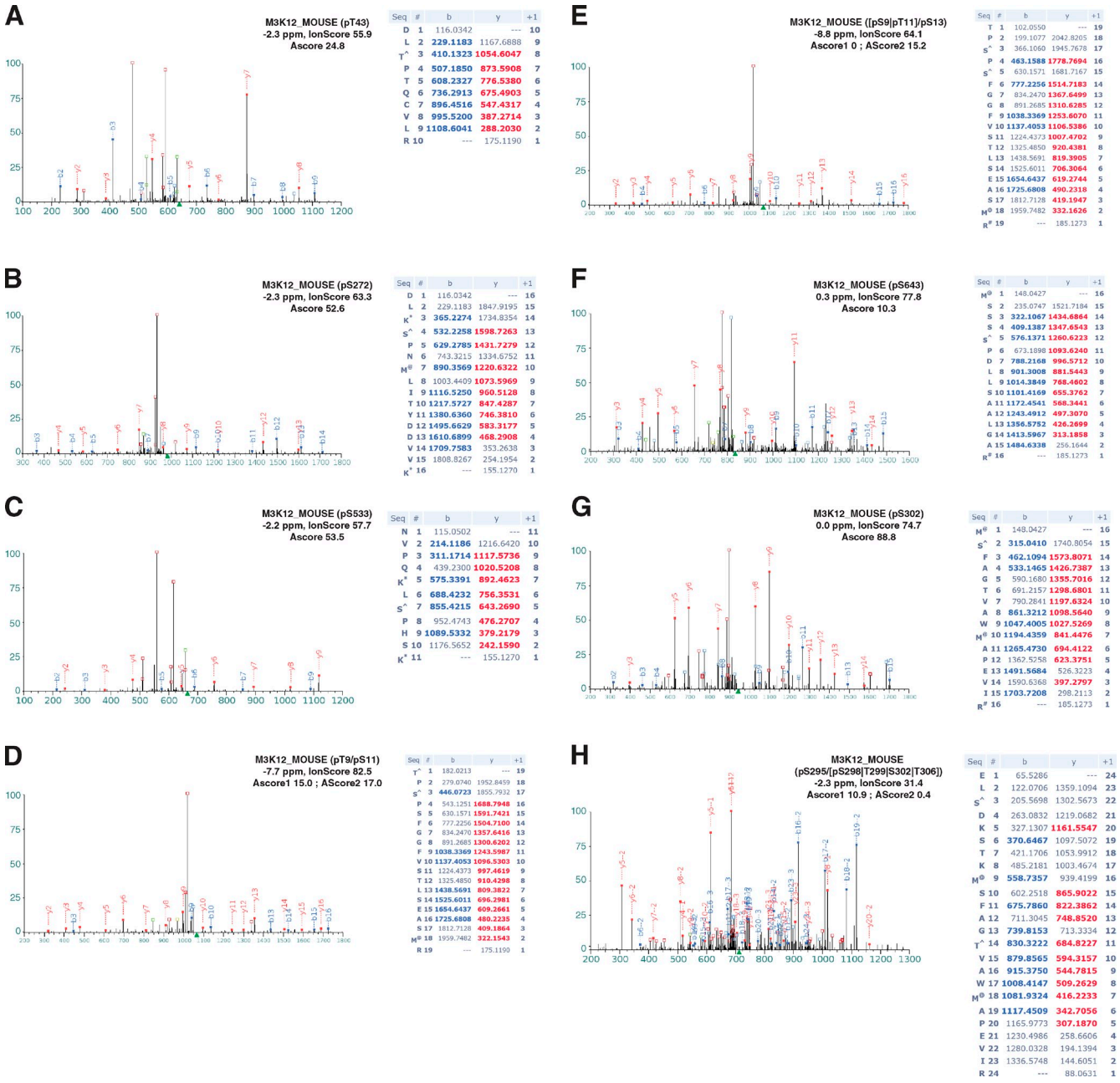

Figure S4. **Peptide spectral matches (PSMs) demonstrating phosphorylation on DLK (M3K12_MOUSE).** The symbol ^ after serine or threonine denotes the position of phosphorylation. Methionine oxidation is denoted by M@, and SILAC-labeled lysine and arginine are indicated as K* and R#, respectively. Matching b- and y-fragment ions are shown in the table and labeled on each spectrum in blue and red, respectively. Open square symbols show commonly observed neutral losses of phosphate (−98 amu) and water (−18 amu) from precursor and fragment ions. (A) PSM matching to the sequence DLT^PTQCVLR from DLK indicates phosphorylation at T43. The precursor ion *m/z* was measured in the full MS spectrum with a mass accuracy of −2.3 ppm and the corresponding MS/MS spectrum was matched by Mascot with an IonScore of 55.9. The Ascore algorithm reports a score of 24.8, indicating that the phosphorylation site has been confidently localized (Ascore >13 denotes 95% confidence) to T43 over T45. (B) PSM showing phosphorylation at S272. (C) PSM showing phosphorylation at S533. (D) PSM demonstrating a multiply phosphorylated sequence with the modifications localized to T9 and S11. (E) Multiply phosphorylated sequence with one modification localized to S13 and the second ambiguously assigned to T9 and/or S11. (F) PSM suggesting phosphorylation at S643. An Ascore of 10.3 represents ∼90% confidence the localization to this residue over S642. Additional confidence in S643 derives from the observation that many DLK phosphorylation sites occur immediately adjacent to proline residues. (G) PSM demonstrating phosphorylation at S302. (H) Confidently identified PSM of a multiply phosphorylated sequence where two Ser and/or Thr modifications reside in the stretch of sequence from S295 to T306, but where site localization cannot be unambiguously assigned.

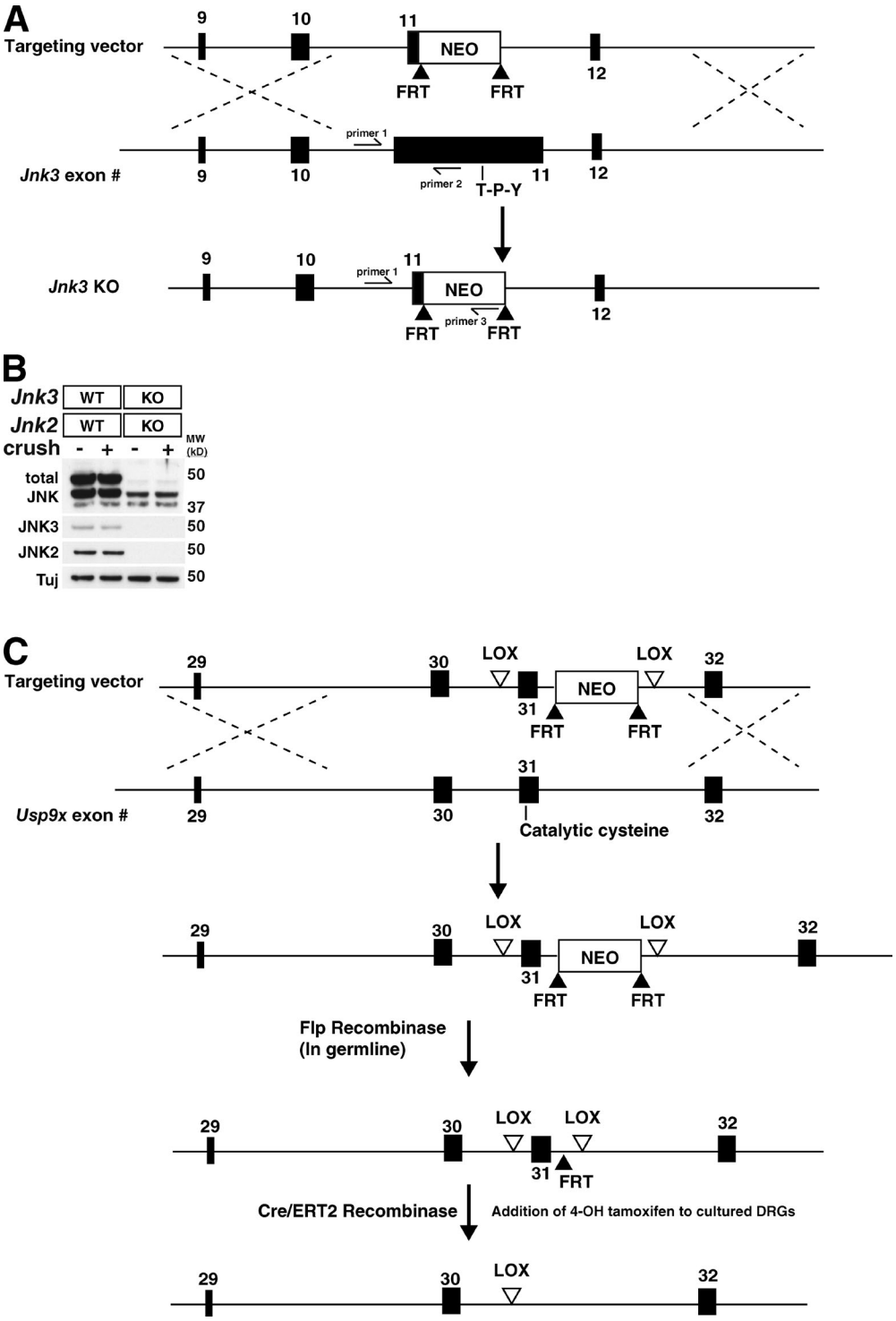

Figure S5. **Generation of *Jnk3* KO and *Usp9x* conditional KO mice.** (A) Illustration of generation of *Jnk3* knockout mice as described in Materials and methods. (B) Western blots for total JNK, JNK2, and JNK3 on retina lysate samples. Loss of immunoreactivity is seen in the *Jnk2/3* double knockout. (C) Illustration of generation of *Usp9x* conditional knockout mice as described in Materials and methods.

References

Borodovsky, A., H. Ovaa, N. Kolli, T. Gan-Erdene, K.D. Wilkinson, H.L. Ploegh, and B.M. Kessler. 2002. Chemistry-based functional proteomics reveals novel members of the deubiquitinating enzyme family. *Chem. Biol.* 9:1149–1159. http://dx.doi.org/10.1016/S1074-5521(02)00248-X